TAPE-DROP TRANSIENT MODEL FOR *IN-SITU* AUTOMATED TAPE PLACEMENT OF THERMOPLASTIC COMPOSITES

Robert C. Costen
NASA Langley Research Center
Hampton, VA

Joseph M. Marchello
Old Dominion University
Norfolk, VA

ABSTRACT

Composite parts of nonuniform thickness can be fabricated by *in-situ* automated tape placement (ATP) if the tape can be started and stopped at interior points of the part instead of always at its edges. This technique is termed start/stop-on-the-part, or, alternatively, tape-add/ tape-drop. The resulting thermal transients need to be managed in order to achieve net shape and maintain uniform interlaminar weld strength and crystallinity. Starting-on-the-part has been treated previously. This paper continues the study with a thermal analysis of stopping-on-the-part.   The thermal source is switched off when the trailing end of the tape enters the nip region of the laydown/consolidation head. The thermal transient is determined by a Fourier-Laplace transform solution of the two-dimensional, time-dependent thermal transport equation. This solution requires that the Peclet number Pe (the dimensionless ratio of inertial to diffusive heat transport) be independent of time and much greater than 1. Plotted isotherms show that the trailing tape-end cools more rapidly than the downstream portions of tape. This cooling can weaken the bond near the tape end; however the length of the affected region is found to be less than 2 mm. To achieve net shape, the consolidation head must continue to move after cut-off until the temperature on the weld interface decreases to the glass transition temperature. The time and elapsed distance for this condition to occur are computed for the Langley ATP robot applying PEEK/carbon fiber composite tape and for two upgrades in robot performance. The elapsed distance after cut-off ranges from about 1 mm for the present robot to about 1 cm for the second upgrade.

KEY WORDS: Modeling, Automated Tape Placement, Thermoplastic Composites, PEEK.

----

1. INTRODUCTION

Carbon fiber/thermoplastic composite tape can be used to fabricate a laminated part by *in-situ* automated tape placement (ATP). In this process, the tape is spooled out and progressively welded under heat and pressure to a previous layer. The steady state ATP process has been modeled extensively, as, for example, in refs. 1-6.

Fabrication of complicated panels may require tape-adds and tape-drops, which are non-steady processes. In a tape-add, a new tape-end is started at an interior point of the panel. This process, also called start-on-the-part, was modeled in ref. 7. The time-dependent, two-dimensional thermal transport equation was solved analytically for a thermal source that switched on at $t = 0$ just as the new tape-end entered the nip region of the laydown/consolidation head. The head started slowly and accelerated in an attempt to compensate for the thermal transient and achieve uniform interlaminar weld strength and crystallinity from the outset. The slow start was also convenient for accurately placing the new tape end. The model implemented the variable head speed by means of a quasi-steady approximation (QSA). A final check, however, showed that the QSA was not valid initially but became valid after a short distance. Consequently, the goal of uniform interlaminar bond strength and crystallinity was not achieved during start-up. However, the length of the non-uniform region was quantified for the present Langley ATP robot and two performance upgrades and found to be less than 1 cm.

The present modeling effort concerns a tape-drop, or stop-on-the-part. The approach is the same as in ref. 7, except that the thermal source is switched *off* at $t = 0$ just as the trailing end of the tape enters the nip region (Fig. 1). Varying the head speed is found to be useless as a means of compensating for the stopping thermal transient, as will be explained. One modeling objective is to determine the length of the region of nonuniform weld strength and crystallinity near the trailing tape-end (the affected length).

The speed of the head remains constant until the temperature on the weld interface decreases to the glass transition temperature T_g. Once this condition is met, consolidation pressure can be released without concern for material springback that would interfere with achieving net shape (the desired design shape). A second objective is to determine the time and elapsed distance from thermal switch-off until the head can be raised from the part.

2. TIME-DEPENDENT MODEL

As mentioned, the stop-on-the-part configuration being modeled is shown in Fig. 1 at $t = 0$ when the trailing end of the tape enters the nip. As the tape-end moves downstream, the consolidation roller conforms around the tape-end to make continuous contact. The model uses a two-dimensional approximation that is valid when the Peclet number $Pe \gg 1$, where Pe is the dimensionless ratio of inertial to diffusive heat transport (ref. 3). The (x, y) coordinate frame is at rest with respect to the head. The origin is located at the nip, where the time-dependent thermal input $q(t)$ (in W m^{-1}) is applied. For $t < 0, q = q_0 = $ const., and for $t \geq 0, q = 0$. The thermal conductivities of the supporting tool and the consolidation head are taken to be the same as the average thermal conductivity of the laminated composite substrate. This idealization makes all the plies thermally equivalent and facilitates an analytic solution. At distances far away from the nip, the temperatures in the tool and in the head are maintained at T_∞ (usually room temperature). Subject to these idealizations, the thermal transport equation is given by

$$\rho C_p \frac{\partial T}{\partial t} + \rho C_p U \frac{\partial T}{\partial x} = K_{11} \frac{\partial^2 T}{\partial x^2} + K_{22} \frac{\partial^2 T}{\partial y^2} + q_0 [1 - H(t)] \delta(x) \delta(y) \qquad (1)$$

where $T(x, y, t)$ is the temperature, ρ is the density, C_p is the specific heat at constant pressure, K_{11} and K_{22} are the tensor thermal conductivity components, $H(t)$ is the Heaviside unit step function, and $\delta(x)$ and $\delta(y)$ are Dirac delta-functions.

In the steady state $(t < 0)$, $T(x, y, t) = T_0(x, y)$, and the thermal input q_0 is constrained so that the temperature on the weld interface $(y = 0)$ decreases passively to the glass transition temperature T_g at the downstream end of the consolidation head x_h. This constraint, which prevents the material from springing back downstream of the consolidation head, is given by

$$T_0(x_h, 0) = T_g \qquad (2)$$

Dimensionless (primed) quantities can be defined as follows:

$$T' \equiv \frac{T - T_\infty}{T_g - T_\infty} \qquad (3a)$$

$$q_0' \equiv \frac{q_0}{2\pi (K_{11} K_{22})^{1/2} (T_g - T_\infty)} \qquad (3b)$$

$$b \equiv \frac{\rho C_p U x_h}{2 K_{11}} = \frac{Pe}{2} \qquad (3c)$$

$$x' \equiv \frac{x}{x_h} \qquad (3d)$$

$$y' \equiv \left(\frac{K_{11}}{K_{22}} \right)^{1/2} \frac{y}{x_h} \qquad (3e)$$

$$t' \equiv \frac{U}{x_h} t \qquad (3f)$$

The partial derivatives then become

$$\frac{\partial}{\partial x} = \frac{1}{x_h} \frac{\partial}{\partial x'} \qquad (3g)$$

$$\frac{\partial}{\partial y} = \frac{1}{x_h} \left(\frac{K_{11}}{K_{22}} \right)^{1/2} \frac{\partial}{\partial y'} \qquad (3h)$$

$$\frac{\partial}{\partial t} = \frac{U}{x_h} \frac{\partial}{\partial t'} \qquad (3i)$$

and (1) becomes

$$2b\frac{\partial T'}{\partial t'}+2b\frac{\partial T'}{\partial x'}=\frac{\partial^2 T'}{\partial x'^2}+\frac{\partial^2 T'}{\partial y'^2}+2\pi\, q_0{}'[1-H(t')]\delta(x')\delta(y')\tag{4}$$

This equation is solvable analytically if b is a constant. Taking the partial t'- derivative gives

$$2b\frac{\partial \tau'}{\partial t'}+2b\frac{\partial \tau'}{\partial x'}=\frac{\partial^2 \tau'}{\partial x'^2}+\frac{\partial^2 \tau'}{\partial y'^2}-2\pi\, q_0{}'\delta(x')\delta(y')\delta(t')\tag{5}$$

where $\tau'\equiv\partial T'/\partial t'$. Equation (5) can now be solved by the method of Fourier and Laplace transforms to give

$$\tau'(x',y',t')=-\frac{q_0{}'}{2t'}\exp\left[-\frac{b}{2}\left(\frac{x'^2+y'^2}{t'}+t'-2x'\right)\right]\tag{6}$$

and

$$T'(x',y',t')=T_o{}'(x',y')-\frac{q_0{}'}{2}\int_0^{t'}\frac{1}{t*}\exp\left[-\frac{b}{2}\left(\frac{x'^2+y'^2}{t*}+t*-2x'\right)\right]dt*\tag{7}$$

where $T_0{}'(x',y')$ is the steady temperature field, and $t*$ is a dummy variable of integration. From references [5] and [7], the steady temperature field is given by

$$T_0{}'(x',y')=q_0{}'\exp(bx')K_0\left[b(x'^2+y'^2)^{1/2}\right]=\frac{q_0{}'}{2}\int_0^{\infty}\frac{1}{t*}\exp\left[-\frac{b}{2}\left(\frac{x'^2+y'^2}{t*}+t*-2x'\right)\right]dt*\tag{8}$$

where K_0 is a hyperbolic Bessel function. The constraint (2) is given in dimensionless variables by

$$T_0{}'(1,0)=1\tag{9}$$

and its application to (8) yields

$$q_0{}'=\frac{1}{\exp(b)K_0(b)}\tag{10}$$

Substituting (8) and (10) into (7) gives finally the dimensionless temperature field for stopping-on-the-part

$$T'(x',y',t')=\frac{\exp(bx')K_0[b(x'^2+y'^2)^{1/2}]}{\exp(b)K_0(b)}\qquad (t'<0)\tag{11a}$$

$$T'(x',y',t')=\frac{1}{2\exp(b)K_0(b)}\int_{t'}^{\infty}\frac{1}{t*}\exp\left[-\frac{b}{2}\left(\frac{x'^2+y'^2}{t*}+t*-2x'\right)\right]dt*\qquad (t'\geq 0)\tag{11b}$$

3. THERMAL TRANSIENT

Equation (11b) can be used to plot the isotherms of dimensionless temperature for various values of b and t' after the thermal switch-off at $t'= 0$. The nature of the thermal transient in the composite substrate during stop-on-the-part is shown in Fig. 2 for $b = 100$. (The thermal state in the head is a mirror image.) For small values of t' (Fig. 2(a)), the isotherms are essentially those of the steady state that existed before switch-off. The movement of the composite from left to right causes the rightward asymmetry. The $T'= 1$ isotherm intersects the weld interface $y'= 0$ at $x'= 1$ -- in agreement with the constraint (9) that the temperature on the weld interface decreases passively to T_g at the downstream end of the consolidation head.

Figure 2(b) shows the isotherms at $t'= 0.001$. At this time, the trailing tape-end is located at $x'= 0.001$. Cooling due to the thermal switch-off has begun. The peak temperature has decreased and the temperature maximum has shifted towards the right to $x'= 0.003$. This shift of the thermal maximum exceeds the movement of the tape, which indicates that the trailing tape-end is cooling faster than the rest of the tape. This rapid cooling could weaken the bond near the tape-end. The physical explanation for this cooling is that the tape-end is located at the interface between the heated composite on the right and the unheated composite on the left. Diffusion will rapidly reduce the high thermal gradient across this interface by causing heat to flow from the hot tape-end to the cool substrate immediately upstream of it.

Figures 2(c) and 2(d) show the isotherms at $t'= 0.01$ and $t'= 0.1$, when the tape end is located at $x'= 0.01$ and $x'= 0.1$, respectively. The thermal maximum continues to decrease and to move to the right somewhat faster than the composite. At $t'= 1$ (not shown), the tape-end exits the consolidation head at $x'= 1$, and the temperature everywhere has already fallen below the glass transition temperature $T_g'= 1$.

A comparison with reference [7] shows that the thermal transient for stopping-on-the-part is not simply the reverse of that for starting-on-the-part. When the thermal source is switched on, the thermal peak stays at the nip $\left(x'= y'= 0 \right)$ as the material heats up. When the thermal source is switched off, the thermal peak moves downstream with the material as cooling occurs. This feature precludes use of varying the head speed to maintain uniform interlaminar weld strength and crystallinity with stopping-on-the-part. The objective of varying the speed is to maintain uniform residence time at temperature in the composite material by speeding up the head as the isotherms enlarge (or, conversely, slowing it down as the isotherms contract). This approach works when the isotherms move with the head, as when starting-on-the-part. It fails when the isotherms move with the material, as when stopping-on-the-part, because changing the head speed will not change the residence time at temperature.

4. CALCULATION PARAMETERS

Sample tape-drop calculations are done for the Langley ATP robot applying PEEK/carbon fiber composite tape. Present operating conditions of the robot correspond to $b \approx 10$. Calculations are also done for two upgrades in robot performance, which correspond to $b = 100$ and $b = 1000$. These upgrades result from proportional increases in the head speed U and consolidation length x_h. Increases in x_h are a natural consequence of making the head more conformable. Relevant temperatures for the ATP process include the composite

degradation temperature T_d and the upper- and lower limits of the crystallization zone, T_{c1} and T_{c0}.

The relevant material parameters are $\rho = 1560\,\text{kg m}^{-3}$, $C_p = 1425\,\text{J kg}^{-1}\,\text{K}^{-1}$, $K_{11} = 6\,\text{W m}^{-1}\,\text{K}^{-1}$, $K_{22} = 0.72\,\text{W m}^{-1}\,\text{K}^{-1}$, $T_d = 823\,\text{K}$, $T_{c1} = 593\,\text{K}$, $T_{c0} = 443\,\text{K}$, and $T_g = 413\,\text{K}$. (The value for T_{c1} is from [6] and for T_{c0} is from [8].) The corresponding dimensionless temperature values are $T_d' = 4.42$, $T_{c1}' = 2.5$, $T_{c0}' = 1.25$, and $T_g' = 1$. The fixed process parameters are $T_\infty = 293\,\text{K}$, tape thickness $d = 1.27 \times 10^{-4}\,\text{m}$, and tape width $w = 3.175 \times 10^{-2}\,\text{m}$.

For the first calculation $(b = 10)$, the input power $Q_0 = wq_0 = 127\,\text{W}$, and the speed and length of the consolidation head are given by $U = 0.0425\,\text{m s}^{-1}$ and $x_h = 1.27 \times 10^{-3}\,\text{m}$. In the second calculation $(b = 100)$, $Q_0 = 397\,\text{W}$, $U = 0.134\,\text{m s}^{-1}$, and $x_h = 4.02 \times 10^{-3}\,\text{m}$. The third calculation $(b = 1000)$ has $Q_0 = 1{,}255\,\text{W}$, $U = 0.425\,\text{m s}^{-1}$, and $x_h = 0.0127\,\text{m}$.

5. LENGTH OF TAPE AFFECTED BY THERMAL SWITCH-OFF

As mentioned, Fig. 2(a) shows essentially the static dimensionless isotherms for $b = 100$. Fig. 2(b) shows the corresponding isotherms at $t' = 0.001$ after thermal switch-off, when the trailing end of the tape is located at $x' = 0.001$. The dimensionless length of tape affected by the cooling due to thermal switch-off can be determined approximately as $\Delta x'_{affected} = 0.009$ by comparing Fig. 2(b) to Fig. 2(a). Figure 2(c) shows the isotherms at $t' = 0.01$, when the tape-end is at $x' = 0.01$. The affected length is now $\Delta x'_{affected} = 0.034$, as determined by comparing again to Fig. 2(a). Figure 2(d) shows the final stages of cooling at $t' = 0.1$, when the tape end is at $x' = 0.1$ and the affected length is $\Delta x'_{affected} = 0.14$. These values and their dimensioned equivalents are given in Table 1, together the corresponding values for $b = 10$ and $b = 1000$. The largest affected length ($\Delta x_{affected} = 1.8\,\text{mm}$) occurs for the second upgrade ($b = 1000$).

Diffusional cooling of the trailing tape-end, as described in this section, suggests that a similar effect can occur along the side edges of the tape. This effect could prematurely cool the side edges and weaken the bond. Although beyond the present scope, this three-dimensional effect needs to be investigated.

6. ELAPSED DISTANCE FOR RELAXATION TO TARGET TEMPERATURE AFTER THERMAL SWITCH-OFF

According to the model, to achieve net shape the consolidation head must continue to move after thermal switch-off until the temperature maximum T_{max} decreases to the glass transition temperature T_g. Equation (11b) can be solved to determine the dimensionless time t' when the maximum dimensionless temperature T'_{max} decreases to $T_g' = 1$. For $b = 1000$, this time is given by $t' = 0.913$, as listed in the right-most column of Table 2. The elapsed distance since switch-off is determined from the dimensionless position of the trailing tape-edge at this time $x'_{trailing\,edge} = 0.913$. In dimensioned units, the elapsed time and distance are given by

$t = 27.3\,\text{ms}$ and $x_{trailing\,edge} = 11.6\,\text{mm}$, as listed in the same column. These values are the largest computed in this study. The elapsed times and distances as $T'_{max} \rightarrow T_g' = 1$ are also given in the same column for $b = 100$ and $b = 10$. Similar computations for other target temperatures, T_d', T_{c1}', and T_{c0}', are summarized in the other columns of the table.

7. CONCLUSIONS

Initially there was hope that the thermal transient that occurs during a tape-drop would affect only the substrate upstream of the trailing tape-end and not the tape itself. Unfortunately, the transient overtakes and cools the tape-end as it moves away under the consolidation head. This cooling, which can weaken the bond, results from the steep thermal gradient created by suddenly switching off the thermal source at the tape-end. Diffusion smoothes out the gradient by causing heat to flow from the hot tape-end to the cool substrate immediately upstream. (Although beyond the present scope, similar diffusional cooling can occur along the side edges of the tape. This three-dimensional effect, which could weaken the bond, needs to be investigated.)

In dealing with the tape-drop thermal transient, there was hope that varying the head speed after thermal switch-off could be used to help compensate, as in the tape-add transient. In the tape-add transient, the isotherms move with the tape head. As the isotherms expand, the head speed can be increased to maintain a constant residence time at temperature in the material. Such a constant residence time can help achieve uniform weld strength and crystallinity. Unfortunately, for a tape-drop, the isotherms after switch-off move with the material instead of the head, so varying the head speed does not help.

The study, consequently, focused on determining the length of tape affected by the cooling transient during a tape-drop. This determination was done graphically by comparing the isotherms at three times during the transient with the steady state isotherms that existed before thermal switch-off. The location of the trailing tape-end at these three times was an important consideration. The affected length was determined for the existing Langley ATP robot applying PEEK/carbon fiber composite tape and for two upgrades in robot performance. The second upgrade had the greatest affected length (1.8 mm).

The study also determined the elapsed time and distance after switch-off before the consolidation head could be lifted from the part without concern for material spring-back. Such spring-back could impede the achievement of net shape. The analytic solution, which requires a constant head speed, was used to compute the elapsed time and distance for the temperature maximum to decrease to the glass transition temperature. The largest computed values occurred for the second upgrade of the Langley robot. The elapsed time was 27 ms and the elapsed distance was 12 mm. Smaller computed values were found for other target temperatures, including the composite degradation temperature and the upper- and lower temperatures of the crystallization zone.

REFERENCES

1. S. Mantell, Q. Wang, and G. S. Springer, *SAMPE International Symposium, 36*, 1763-1772 (1996).
2. J. A. Hinkley, J. M. Marchello, and B. C. Messier, NASA TM-110203 (1996).

3. R. Pitchumani, R. C. Don, J. W. Gillespie, Jr., and S. Ranganathan in V. Prasad *et al.*, eds., *HTD-Vol. 289*, *Thermal Processing of Materials: Thermal Mechanics, Controls and Composites,* ASME, 223-234 (1994).
4. R. G. Irwin, Jr. and S. I. Güçeri, *AMD-Vol. 194, Mechanics in Materials Processing and Manufacturing*, ASME, 319-333 (1994).
5. R. C. Costen and J. M. Marchello, *SAMPE International Symposium, 42*, 33-47 (1997).
6. F. O. Sonmez and H. T. Hahn, *J. Thermoplastic Composite Materials, 10*, 198-240 (1997).
7. R. C. Costen and J. M. Marchello, *SAMPE International Symposium, 43*, 2005-2019 (1998).
8. W. J. Unger and J. S. Hansen, *J. Composite Materials, 27*, 59-82 (1993)

BIOGRAPHIES

Robert C. Costen is an applied mathematician at NASA-Langley who works in the Composites and Polymers Branch. He has authored and co-authored numerous modeling papers in materials processing, aerodynamics, atmospheric science, lasers, and radiation protection.

Joseph M. Marchello is a professor of civil and mechanical engineering at Old Dominion University. He is a chemical engineer with over 30 years of teaching and research experience in process development. He is author of over 100 technical and scientific papers.

Table 1. Length of tape affected by thermal switch-off $\Delta x_{affected}$.

$t' = x'_{trailing\ edge}$		0.001	0.01	0.1
t , ms		0.030	0.30	3.0
$b = 10$	$x_{trailing\ edge}$, mm	0.0013	0.013	0.13
	$\Delta x'_{affected}$	0.023	0.08	0.14
	$\Delta x_{affected}$, mm	0.029	0.10	0.18
$b = 100$	$x_{trailing\ edge}$, mm	0.0040	0.040	0.40
	$\Delta x'_{affected}$	0.009	0.034	0.14
	$\Delta x_{affected}$, mm	0.036	0.14	0.56
$b = 1000$	$x_{trailing\ edge}$, mm	0.013	0.13	1.3
	$\Delta x'_{affected}$	0.0044	0.014	0.14
	$\Delta x_{affected}$, mm	0.056	0.18	1.8

Table 2. Elapsed distance $x_{trailing\ edge}$ for relaxation to target temperature.

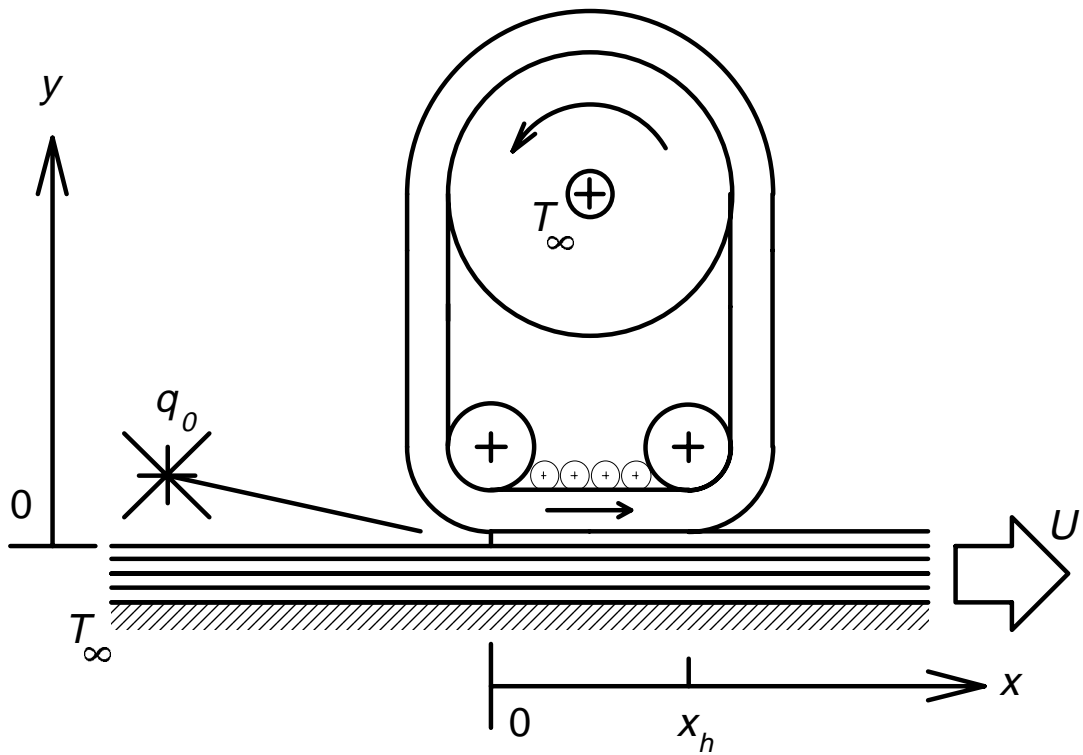|		$T'_{max} \to T_d'$ = 4.42	$T'_{max} \to T_{c1}$ = 2.5	$T'_{max} \to T_{c0}$ = 1.25	$T'_{max} \to T_g$ = 1
$b = 10$	$t' = x'_{trailing\ edge}$	0.00486	0.0400	0.296	0.529
	t, ms	0.145	1.20	8.84	15.8
	$x_{trailing\ edge}$, mm	0.00617	0.0508	0.376	0.672
$b = 100$	$t' = x'_{trailing\ edge}$	0.0213	0.0927	0.473	0.780
	t, ms	0.636	2.77	14.1	23.3
	$x_{trailing\ edge}$, mm	0.0855	0.372	1.90	3.13
$b = 1000$	$t' = x'_{trailing\ edge}$	0.0367	0.154	0.573	0.913
	t, ms	1.10	4.60	17.1	27.3
	$x_{trailing\ edge}$, mm	0.466	1.96	7.28	11.6

Figure 1. Stop-on-the-part configuration at $t = 0$, when the trailing tape-end enters the nip and the thermal source q_0 is switched off.
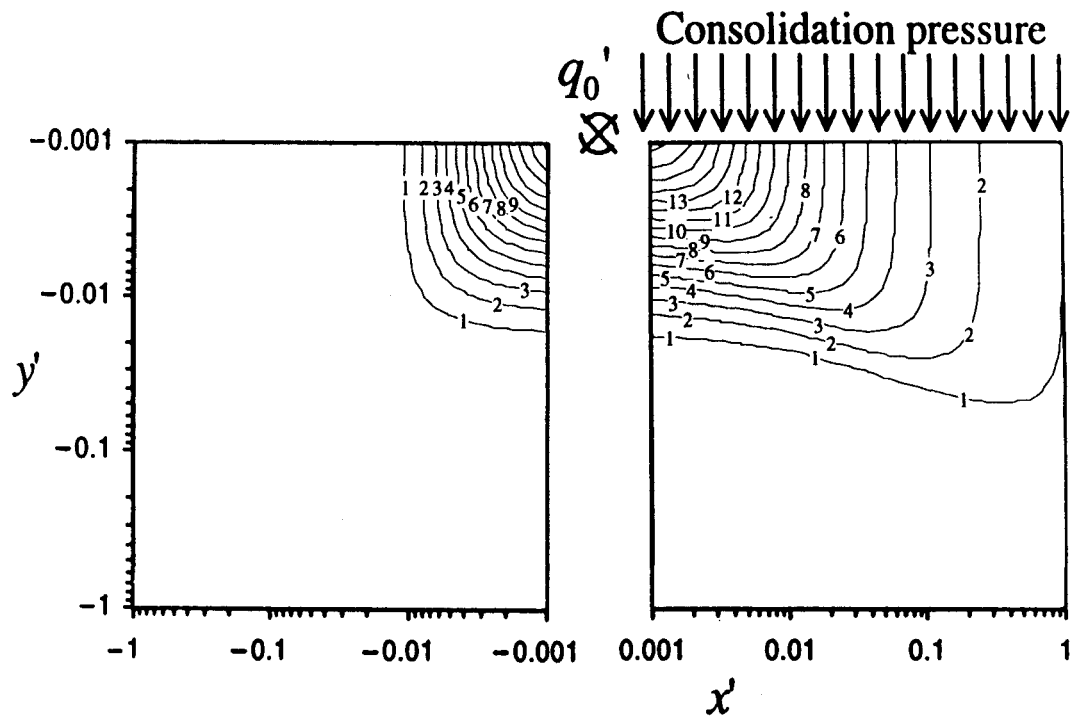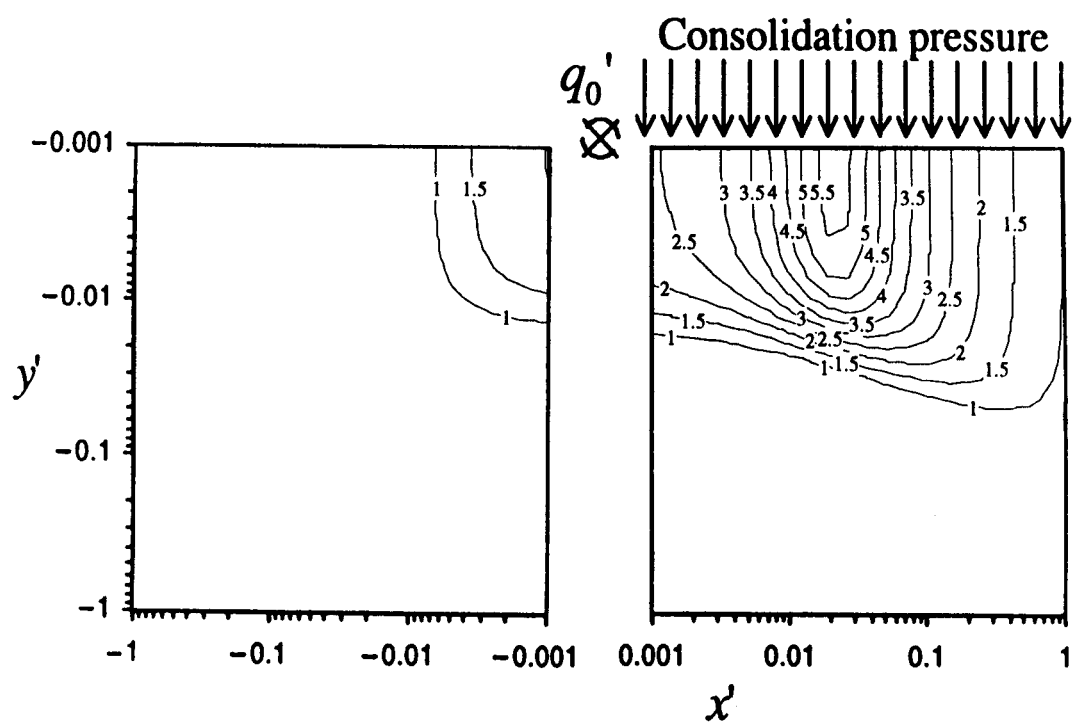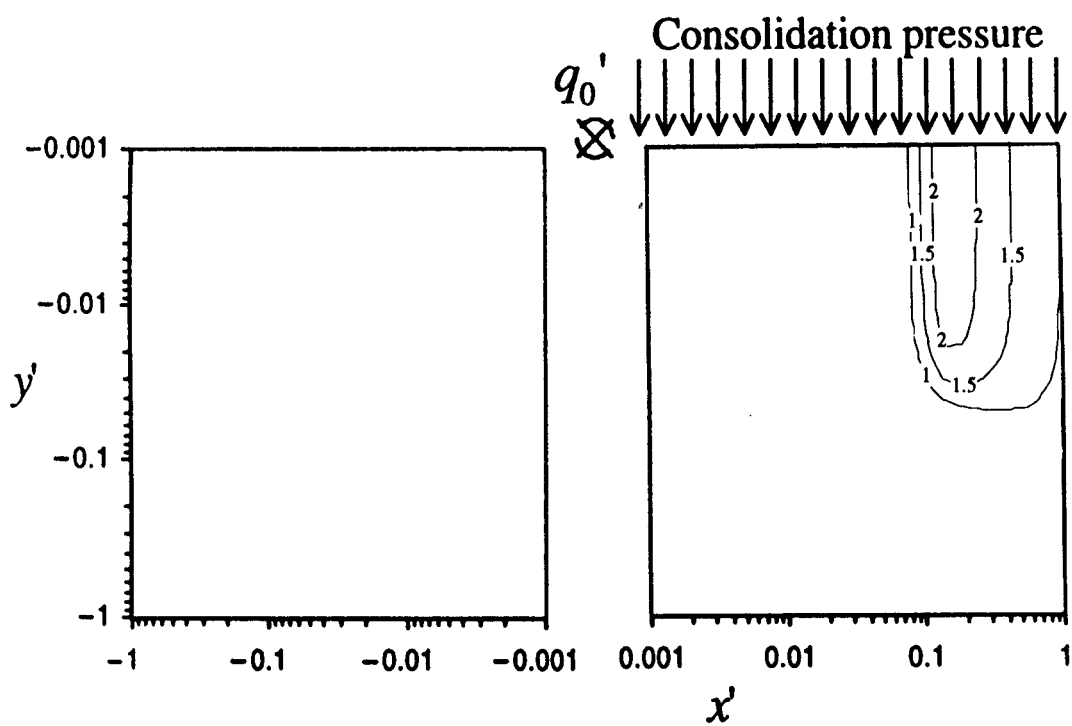
(a) $t' = 0.0001$

Figure 2. Isotherms of dimensionless temperature T' in composite substrate for $b = \text{Pe}/2 = 100$ and various dimensionless times t' during stop-on-the-part. The thermal source q_0' is switched off at $t' = 0$.
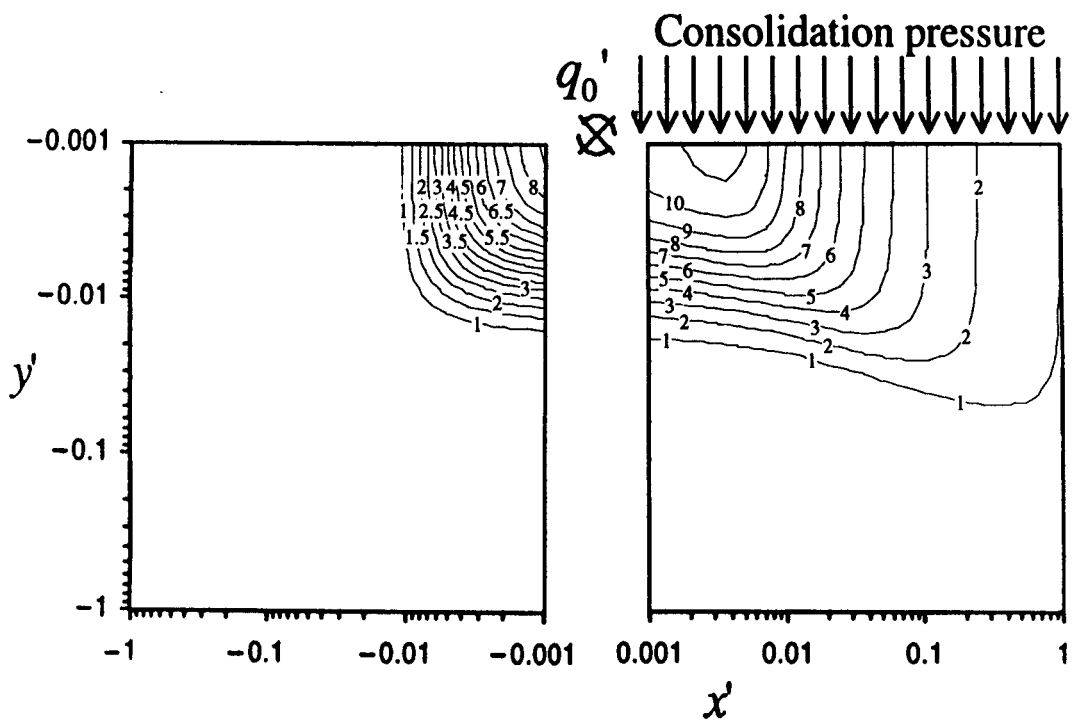
(b) $t' = 0.001$

(c) $t' = 0.01$

(d) $t' = 0.1$

Figure 2. Concluded